Iranian Journal of Organic Chemistry Vol. 10, No. 4 (2018) 2457-2465

Structural and spectral (IR, UV-Vis, CD and DOS) properties of active substance d,l-HMPAO and its complex with technetium-99m radionuclide ^{99m}Tc-exametazime

Mehdi Nabati*

Synthesis and Molecular Simulation Laboratory, Chemistry Department, Pars Isotope Company, P.O. Box: 1437663181, Tehran, Iran

Received: August 2018; Revised: August 2018; Accepted: October 2018

Abstract: During the present study, the structural (bond angles, bond lengths, bond orders and natural bond orbital population), spectral (IR, UV-Vis and CD) properties of the active substance d,l-hexamethylpropylene amineoxime (d,l-HMPAO) and its complex with technetium-99m radionuclide ^{99m}Tc-d,l-HMPAO are discussed by the density functional theory (DFT) calculations with B3LYP functional and cc-pVDZ basis set of theory in gas phase at room temperature. The Lanl2DZ basis set is used to computation of the technetium atom. Also, the quantum chemical properties such as frontier molecular orbitals (FMOs) energies (E_{HOMO} and E_{LUMO}), the energy gap, molecular electrostatic potential (MEP) graph and the density of states (DOS) are investigated. The theoretical UV-Vis bands of ^{99m}Tc-d,l-HMPAO radiopharmaceutical are at 405, 404 and 471 nm. The circular dichroism (CD) spectrum indicates this nuclear medicine is a right-handed molecule.

Keywords: DFT study, Exametazime, HMPAO, Nuclear medicine, Radiopharmaceutical, Reactivity, Stability.

Introduction

A nuclear medicine or radiopharmaceutical is a drug that can be used either for therapeutic or diagnostic aims [1-4]. It is made from two parts: an organic compound and a radionuclide or radioisotope [5-7]. The duty of the organic molecular structure is delivery of the radionuclide to specific organs, tissues and or cells [8-10]. Each radionuclide has own special properties and applications [11-16]. The radionuclides technetium-99m (^{99m}Tc), iodine-123 (^{123}I), iodine-131 (^{131}I), thallium-201 (^{201}Tl), indium-111 (^{111}In) and fluorine-18 (^{18}F) are used for diagnostic (imaging) purposes [17-22]. These radioisotopes emit gamma rays [23].

The gamma rays are detected by Single Photon Emission Computed Tomography (SPECT) or Positron Emission Tomography (PET) cameras [24, 25]. Radiolabelled organic compounds production requires pharmaceutical industry expertise with specific conditions of nuclear facility. The important facilities for manufacturing of nuclear medicines are located in North America and Europe [26-28]. Thecnetium-99m radionuclide is the most widely used radiotracer in diagnostic radiopharmaceuticals [29]. The technetium-99m radiopharmaceuticals can be used to diagnosis of various diseases such as certain types of cancers [30]. For instance, technetium-99m exametazime (^{99m}Tc-d,l-HMPAO) is widely used to detect the altered regional cerebral perfusion in stroke and other cerebrovascular diseases [31-34]. Firstly, this radiopharmaceutical has been introduced as a tracer for brain imaging studies in humans as early as 1985 and its diagnostic utility has

*Corresponding author: Tel: +98 21 88337023; Fax.: +98 21 88337024; E-mail: mnabati@ymail.com

been very well documented [35]. Currently, this nuclear medicine is recommended for brain perfusion studies using SPECT camera by European Association of Nuclear Medicine (EANM) [36]. The active substance, ligand hexamethylpropylene amineoxime (HMPAO) has two chiral centers [37]. So, it is in three diastereomers: meso (R,S), d (R,R) and l (S,S). The d,l-complex revealed high brain uptake and retention compared to the meso-complex [38]. Consequently, the technetium-99m-exametazime is specified as radiochemical impurity in the technetium-99m-HMPAO injection monograph. Nowadays, more studies are done about clinically properties of this nuclear medicine [39-42], but its chemical properties haven't been discussed completely. So, the present study is related to the discussion of the structural and spectral properties of d,l-HMPAO and its complex with technetium-99m radioisotope by density functional theory (DFT) computational method.

Results and discussion

Scheme **1** shows the molecular structure of d,l-HMPAO molecule and its complex with technetium-99m radioisotope ^{99m}Tc-d,l-HMPAO. During the present study, the structural and spectral (IR, UV-Vis and CD) properties, reactivity and stability of the mentioned compounds are discussed. It is necessary to say that all our findings have been done based on the theoretically methods.

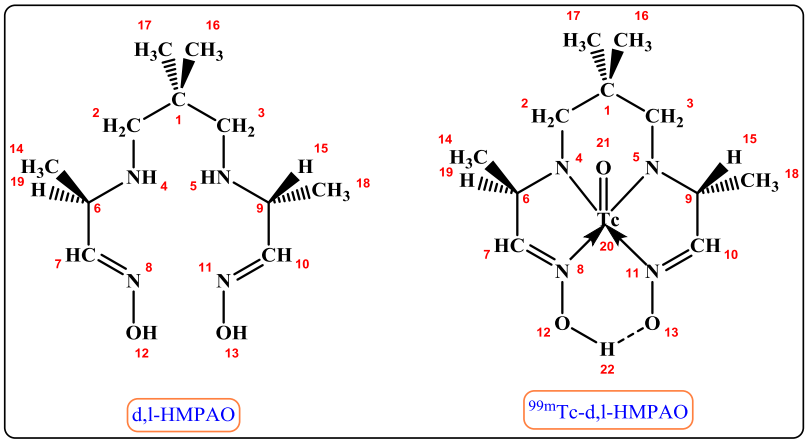

Scheme 1: The molecular structures of d,l-HMPAO and ^{99m}Tc-d,l-HMPAO compounds.

Structural properties of d,l-HMPAO and ^{99m}Tc-d,l-HMPAO compounds

In first step, the studied molecular structures were optimized by density functional theory (DFT) computational method. The optimized molecular structures are indicated in Figure **1**.

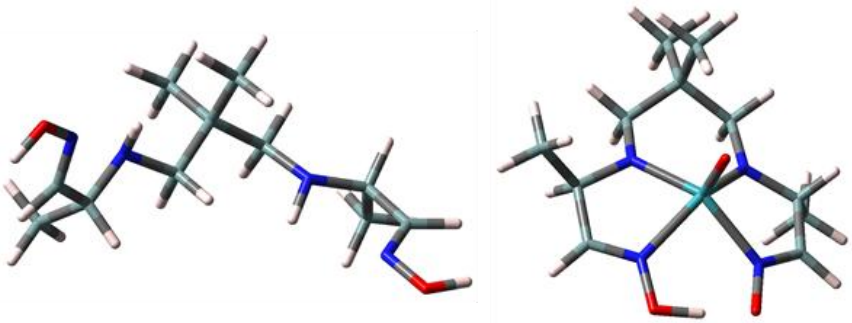

Figure 1. The optimized structures of d,l-HMPAO and ^{99m}Tc-d,l-HMPAO compounds.

The bond lengths, bond angles and bond orders data of ^{99m}Tc-d,l-HMPAO complex has been collected in Table **1**. As can be seen from the data, the Tc=O bond shows bond length 1.693 Å and bond order (B.O.) 1.712. The bond lengths between technetium-99m and nitrogen atoms of ligand are between 1.942 Å and 2.136 Å and the bond lengths between technetium-99m radionuclide and N8 and N11 atoms are longer than the Tc20-N4 andTc20-N5 bond lengths. This happens due to the nature of these bonds. The Tc20-N4 andTc20-N5 bonds are composed by dative electrons of the nitrogen atoms. So, these bonds are week and the bond orders data proves that. From the data of the Table **1**, the Tc20-N8 and Tc20-N11 bond orders amounts are lower than the Tc20-N4 and Tc20-N5 ones.

Table 1: Bond lengths, bond angles and bond orders data of ^{99m}Tc-d,l-HMPAO compound.

Bonds	Bond length (Å)	Bond order (B.O.)	Bond angle	Angle (degree)
Tc20-O21	1.693	1.712	N4-Tc20-O21	110.046
N4-Tc20	1.955	0.815	N5-Tc20-O21	110.445
N5-Tc20	1.942	0.857	N8-Tc20-O21	112.214
N8-Tc20	2.136	0.398	N11-Tc20-O21	107.268
N11-Tc20	2.113	0.439	N4-Tc20-N5	91.380
O12-H22	1.101	0.474	N5-Tc20-N11	78.957
O13-H22 (hydrogen bond)	1.357	0.259	N11-Tc20-N8	84.990
N8-O12	1.334	1.114	N8-Tc20-N4	77.810
N11-O13	1.306	1.184	O12-H22-O13	169.690

Also, we can see that a hydrogen bond is composed between oxygen-13 and hydrogen-22 atoms with bond order 0.259. The three atoms O12, H22 and O13 are in a line (O12-H22-O13 bond angle = 170 degree). On the other hand, the N-Tc-O bond angles are longer than the N-Tc-N ones. So, the Tc=O core composes square pyramidal geometry with the nitrogen atoms of the ligand.

Table **2** has been collected the natural bond orbitals (NBOs) population analysis data of ^{99m}Tc-d,l-HMPAO compound. From the data of the Table **2**, more d orbitals of technetium atom participate in composition of Tc-O and Tc-N bond orbitals. In contrast, the oxygen and nitrogen atoms use more p orbitals in composition of these bonds. Approximately, the lone pair electrons of technetium, oxygen and nitrogen atoms are in d, s and p orbitals, respectively. Also, we can see the N8 and N11 atoms don't have lone pair electrons because they use the lone pair electrons to composition the bond with Tc=O core by dative bond formation mean.

The charges on the atoms of d,l-HMPAO and ^{99m}Tc-d,l-HMPAO compounds are collected in Table **3**. It can be seen from the data of the Table 3 that the charge on technetium-99m radionuclide is +1. By comparison of charges on the nitrogen atoms of d,l-HMPAO molecule and technetium-99m-d,l-HMPAO complex, we see the nitrogen atoms connected to the technetium-99m radionuclide have more negative charge. This is due to the more electronegativity property of nitrogen atoms to technetium-99m radioisotope.

Reactivity prediction of d,l-HMPAO and ^{99m}Tc-d,l-HMPAO compounds

Frontier molecular orbitals (FMOs) analysis can give good information about the reactivity and stability of the organic and inorganic compounds [43-48]. FMOs are called to the highest occupied molecular orbital (HOMO) and lowest unoccupied molecular orbital (LUMO) [49]. Figure **2** shows the frontier molecular orbitals (HOMO and LUMO) of d,l-HMPAO and ^{99m}Tc-d,l-HMPAO compounds. It can be seen from the graphs, the HOMO orbital of the d,l-HMPAO molecule is located on the N4 and N5 atoms. In contrast, the N8 and N11 atoms have more roles in construction of the LUMO orbital. On the other hand, the main part of the LUMO orbital of the technetium-99m-d,l-HMPAO complex has been made by Tc=O

core. The data of the energies of these frontier molecular orbitals have been collected in Table 4. It can be deduced from the data of the Table 4 that the technetium complex of d,l-HMPAO has low stability than the active substance d,l-HMPAO. The more stability of d,l-HMPAO molecule is due to its high

Table 2: Natural bond orbitals (NBOs) analysis data of ^{99m}Tc-d,l-HMPAO compound.

Bonds	Occupancy	Population/Bond orbital/Hybrids
σ(Tc20-O21)	1.81052	16.92% Tc20 ($sp^{99.99}d^{99.99}$), 83.08% O21 ($sp^{99.99}d^{0.35}$)
π1(Tc20-O21)	1.95997	29.57% Tc20 ($sp^{0.06}d^{6.24}$), 70.43% O21 ($sp^{4.77}d^{0.01}$)
π2(Tc20-O21)	1.77556	19.81% Tc20 ($sp^{4.89}d^{14.95}$), 80.19% O21 ($sp^{99.99}d^{0.75}$)
σ(Tc20-N4)	1.81562	17.10% Tc20 ($sp^{0.87}d^{2.47}$), 82.90% N4 ($sp^{2.21}$)
σ(Tc20-N5)	1.81557	17.79% Tc20 ($sp^{0.82}d^{2.71}$), 82.21% N5 ($sp^{2.25}$)
σ(Tc20-N8)	1.86465	12.63% Tc20 ($sp^{0.71}d^{2.35}$), 87.37% N8 ($sp^{2.39}$)
σ(Tc20-N11)	1.84275	14.28% Tc20 ($sp^{0.89}d^{2.43}$), 85.72% N11 ($sp^{2.72}$)
LP(Tc20)	1.94569	Tc20 ($sp^{0.37}d^{99.99}$)
LP(O21)	1.96522	O21 ($sp^{0.21}$)
LP(N4)	1.63681	N4 ($sp^{99.99}d^{0.02}$)
LP(N5)	1.62094	N5 ($sp^{99.99}d^{0.01}$)

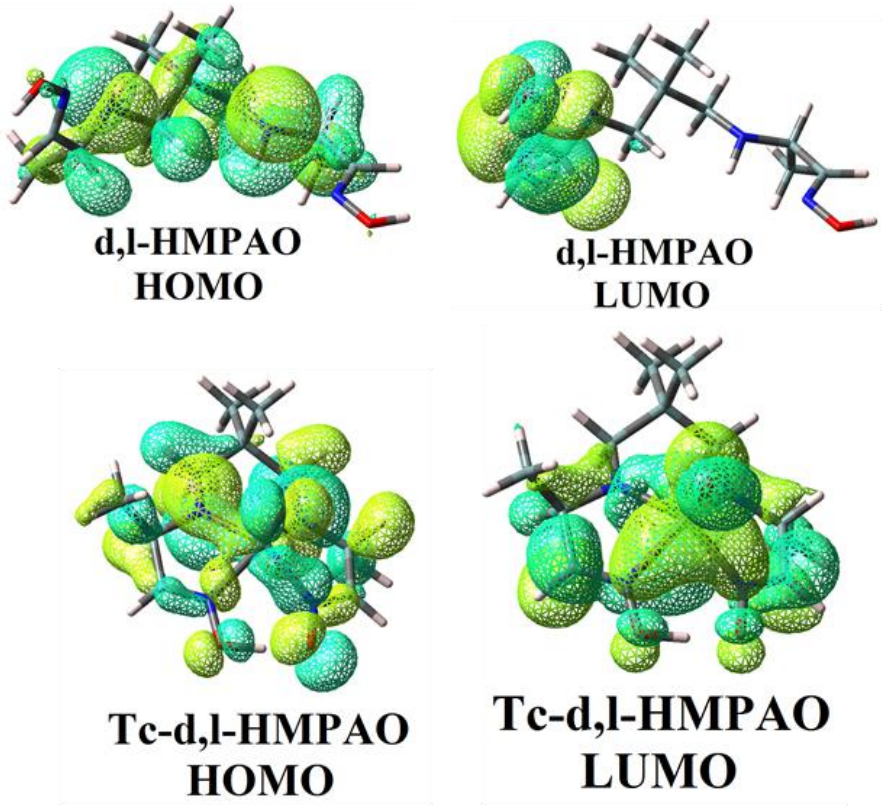

Figure 2: The frontier molecular orbitals of d,l-HMPAO and ^{99m}Tc-d,l-HMPAO compounds.

HOMO/LUMO energies gap. This active substance and its complex with technetium-99m radionuclide have identical HOMO energy, but the LOMO energy of ^{99m}Tc-exametazime compound is lower than the d,l-

HMPAO molecule. So, the ^{99m}Tc-exametazime nuclear medicine has more reactivity and it is an unstable compound. The density of states (DOS) graphs (Figure **3**) indicates clearly the differences in energies of the frontier molecular orbitals of the d,l-HMPAO and ^{99m}Tc-d,l-HMPAO compounds. Figure **4** shows the molecular electrostatic potential (MEP) graphs of d,l-HMPAO and ^{99m}Tc-d,l-HMPAO compounds. We can see from these graphs that low stability and more reactivity of ^{99m}Tc-exametazime radiopharmaceutical

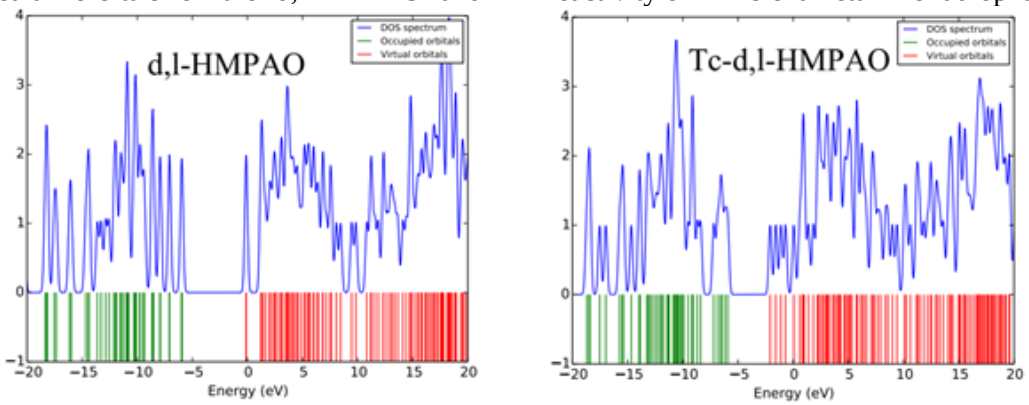

Figure 3: The density of states (DOS) graphs of d,l-HMPAO and ^{99m}Tc-d,l-HMPAO compounds.

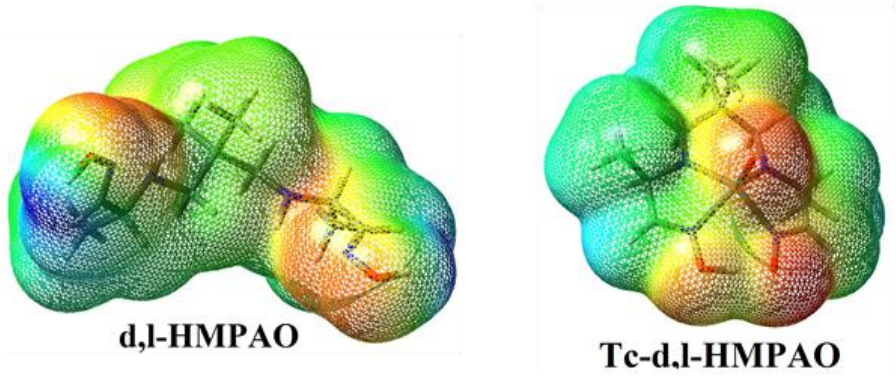

Figure 4: The molecular electrostatic potential (MEP) graphs of d,l-HMPAO and ^{99m}Tc-d,l-HMPAO compounds.

is due to its Tc=O core. It is necessary to say that the blue and red loops of the MEP graphs are related to the electron-poor and electron-rich parts of the molecular structures, respectively.

Spectral study of d,l-HMPAO and ^{99m}Tc-d,l-HMPAO compounds

Chemical analysis and identification of real structure of radiopharmaceuticals are more difficult due to the low half time of the radioisotopes [50-52]. So, the theoretical spectral study of nuclear medicines can give us important information about their structures. During this part of the article, CD, UV-Vis and IR spectra of the studied compounds will be discussed.

Figure **5** shows the circular dichroism (CD) spectra of d,l-HMPAO and ^{99m}Tc-d,l-HMPAO compounds. It can be easily seen from the CD spectra, the d,l-HMPAO and ^{99m}Tc-d,l-HMPAO molecules have the left- and right-handed structures, respectively. So, the participation of the technetium radionuclide in reaction with active substance can be easily identified by CD spectroscopy.

The UV-Vis spectra of d,l-HMPAO and ^{99m}Tc-d,l-HMPAO compounds have been shown in Figure 6.

D,L-HMPAO: UV-Vis [wavelength of electronic transition (nm), energies (cm^{-1}), electronic transitions]:

a. 254.090 nm (39356.095 cm^{-1}), HOMO-1 to LUMO+1 (29%) and HOMO to LUMO+1 (70%)

b. 252.821 nm (39553.702 cm^{-1}), HOMO-1 to LUMO (58%) and HOMO to LUMO (41%)
c. 230.110 nm (43457.453 cm^{-1}), HOMO-1 to LUMO (41%) and HOMO to LUMO (59%)
^{99m}Tc-d,l-HMPAO: UV-Vis [wavelength of electronic transition (nm), energies (cm^{-1}), electronic transitions]:
a. 471.061 nm (21228.659 cm^{-1}), HOMO-2 to LUMO (34%), HOMO-1 to LUMO (29%), HOMO to LUMO (16%), HOMO-3 to LUMO (5%) and HOMO-2 to LUMO+2 (2%)

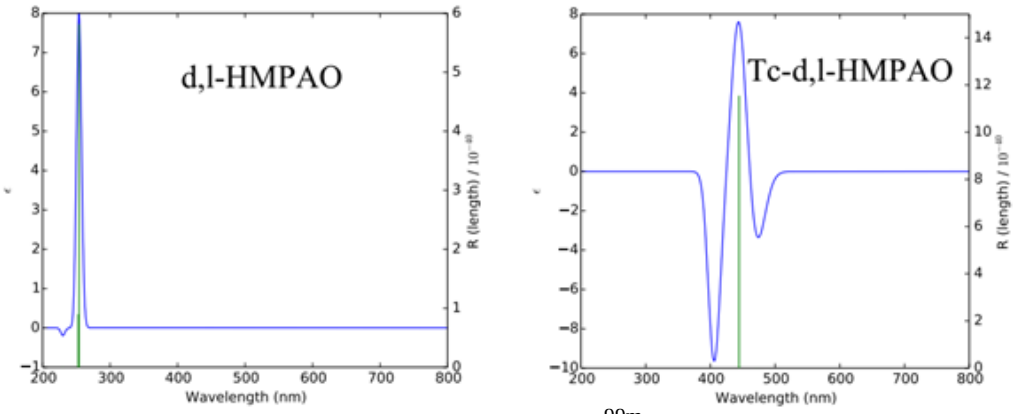

Figure 5: The CD spectra of d,l-HMPAO and ^{99m}Tc-d,l-HMPAO compounds.

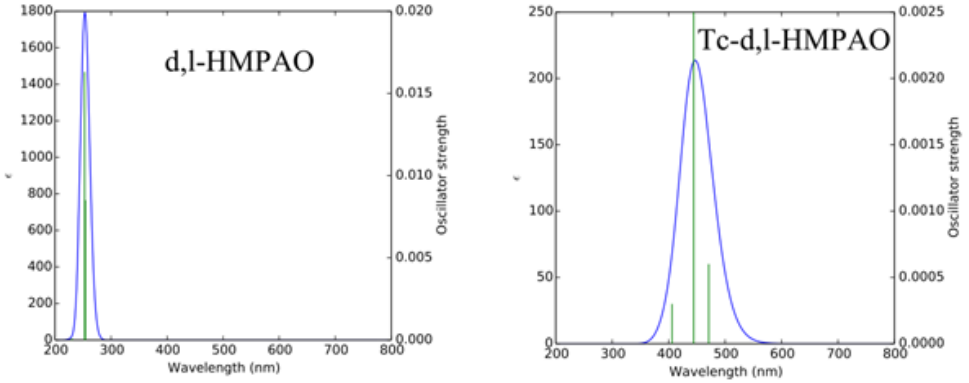

Figure 6: The UV-Vis spectra of d,l-HMPAO and ^{99m}Tc-d,l-HMPAO compounds.

b. 444.321 nm (22506.250 cm^{-1}), HOMO to LUMO (78%), HOMO-1 to LUMO (7%) and HOMO-2 to LUMO (7%)
c. 405.930 nm (24634.762 cm^{-1}), HOMO-2 to LUMO+1 (39%), HOMO-1 to LUMO+1 (34%), HOMO-3 to LUMO+1 (7%) and HOMO to LUMO+1 (4%)
Figure **7** shows the IR spectra of the molecular structures under study. Here, the main harmonic frequencies (cm^{-1}) of the structures are discussed.

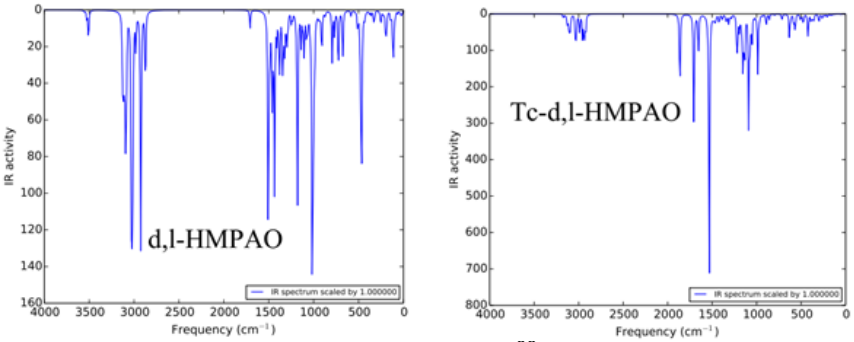

Figure 7: The IR spectra of d,l-HMPAO and ^{99m}Tc-d,l-HMPAO compounds.

Table 3: The charges on the atoms of d,l-HMPAO and ^{99m}Tc-d,l-HMPAO compounds.

Atoms	d,l-HMPAO	^{99m}Tc-d,l-HMPAO
Tc20	-	1.052
O21	-	-0.433
N4	-0.191	-0.509
N5	-0.197	-0.518
N8	-0.067	-0.171
N11	-0.055	-0.143

Table 4. The frontier molecular orbitals energies data of d,l-HMPAO and ^{99m}Tc-d,l-HMPAO compounds.

Compounds	HOMO (eV)	LUMO (eV)	GAP (eV)
d,l-HMPAO	-5.93	-0.12	5.81
^{99m}Tc-d,l-HMPAO	-5.93	-2.09	3.84

D,L-HMPAO: 15.621, 22.011, 34.703, 47.522, 63.401, 92.446, 106.001, 110.526, 118.585, 141.143, 182.239, 190.083, 200.376, 219.960, 228.613, 246.202, 251.589, 253.222, 266.390, 294.562, 325.442, 336.460, 360.590, 379.389, 422.331, 434.325, 456.229, 464.718, 470.928, 483.607, 492.186, 510.048, 584.063, 673.295, 676.691, 724.933, 768.124, 793.730, 869.493, 877.011, 904.734, 906.546, 914.154, 928.903, 934.451, 947.636, 962.123, 971.259, 990.177, 1006.335, 1017.473, 1037.449, 1064.062, 1076.801, 1082.985, 1105.093, 1118.522, 1140.1984, 1178.613, 1186.810, 1205.558, 1236.903, 1249.438, 1287.126, 1298.757, 1300.558, 1311.765, 1324.400, 1331.443, 1343.215, 1349.051, 1373.974, 1377.113, 1378.629, 1385.439, 1391.694, 1410.316, 1434.952, 1435.408, 1453.396, 1455.878, 1458.668, 1460.510, 1465.875, 1466.903, 1472.558, 1478.273, 1486.429, 1491.781, 1503.252, 1508.230, 1708.129, 1709.041, 2873.911, 2922.750, 2925.789, 2980.329, 3013.409, 3018.146, 3019.789, 3023.152, 3025.745, 3027.842, 3031.610, 3033.088, 3084.239, 3091.724, 3096.896, 3106.811, 3116.213, 3122.620, 3123.999, 3130.067, 3507.561, 3526.835, 3554.265, and 3559.626.

^{99m}Tc-d,l-HMPAO: 52.264, 62.939, 84.412, 108.607, 126.889, 142.592, 159.236, 174.481, 180.140, 198.816, 208.369, 229.790, 233.529, 241.382, 260.278, 261.883, 272.247, 280.577, 300.036, 304.559, 351.496, 357.181, 372.591, 388.761, 390.415, 418.216, 422.769, 429.300, 467.059, 477.198, 496.442, 409.401, 466.608, 582.415, 616.444, 631.486, 702.228, 716.270, 797.435, 857.919, 890.379, 892.471, 894.326, 928.151, 932.389, 944.657, 947.271, 962.618, 968.995, 986.383, 1009.709, 1025.424, 1052.169, 1064.225, 1073.225, 1074.248, 1089.459, 1132.140, 1137.542, 1151.599, 1158.428, 1172.995, 1193.121, 1210.011, 1221.506, 1227.812, 1280.433, 1283.271, 1295.531, 1303.319, 1314.564, 1332.252, 1341.994, 1351.198, 1381.278, 1382.888, 1384.624, 1387.235, 1393.658, 1423.270, 1455.148, 1455.300, 1459.110, 1461.668, 1463.945, 1467.046, 1472.413, 1476.895, 1480.825,

1487.859, 1532.919, 1653.978, 1704.980, 1862.880, 2919.878, 2931.111, 2938..489, 2956.371, 2986.704, 2992.349, 3023.354, 3030.463, 3035.826, 3038.518, 3088.401, 3096.058, 3100.984, 3111.953, 3112.935, 3128.735, 3129.124, 3150.605, 3169.286, and 3172.156.

Conclusions

During the present study, the structural and spectral (UV-Vis, IR and CD) properties, stability and reactivity of the active substance d,l-HMPAO and its complex with the technetium-99m radioisotope are discussed. All discussions and investigations have been done based on theoretical studies. The molecular structures have been optimized in the gas phase at B3LYP/cc-pVDZ level of theory. The technetium atom of the nuclear medicine under study has been computed with Lanl2DZ basis set of theory. It can be deduced from the discussion about the studied structures that the Tc=O core composes square pyramidal geometry with the nitrogen atoms of the active substance. Also, our calculations show the stability of the technetium complex is lower than the active substance.

Computational method

During present research, all calculations were carried out by Gaussian 03 package [53] using density functional theory (DFT) computational method by B3LYP functional with cc-pVDZ basis set. The Lanl2DZ basis set was used for the technetium-99m radionuclide. The computations were done in the gas phase at room temperature. It wasn't shown any imaginary frequency in IR computation for the molecular structures. It proves accuracy of our computations.

Acknowledgements

The corresponding author is grateful to Mr. Hossein Abbasi for providing valuable suggestions

References

[1] Ayaz, S. *J. Clin. Anal. Med.*, **2017**, *8*, 14-18.
[2] Erfani, M.; TShafiei, M. *Nucl. Med. Biol.*, **2014**, *30*, 317-321.
[3] Erfani, M.; TShafiei, M.; Charkhlooie, G.; Goudarzi, M. *Iran J. Nucl. Med.*, **2015**, *23*, 15-20.
[4] Fischer, S.; Hiller, A.; Smits, R.; Hoepping, A.; Funke, U.; Wenzel, B.; Cumming, P.; Sabri, O.; Steinbach, J.; Brust, P. *Appl. Radiat. Isot.*, **2013**, *74*, 128-136.
[5] Nabati, M.; Kermanian, M.; Mohammadnejad-Mehrabani, H.; Kafshboran, H. R.; Mehmannavaz, M.; Sarshar, S. *Chem. Method.*, **2018**, *3*, 85-99.
[6] Eckelman, W. C.; Windhorst, A. D.; O'Hara, C. *Nucl. Med. Biol.*, **2017**, *55*, 47-48.
[7] Chiesa, C.; Gleisner, K. S.; Flux, G.; Gear, J.; Walrand, S.; Bacher, K.; Eberlein, U.; Visser, E. P.; Chouin, N.; Ljungberg, M.; Bardies, M.; Lassmann, M.; Strigari, L.; Konijnenberg, M. W. *Eur. J. Nucl. Med. Mol. Imaging*, **2017**, *44*, 1783-1786.
[8] Kennedy-Dixon, T.; Gossell-Williams, M.; Cooper, M.; Trabelsi, M.; Vinjamuri, S. *J. Nucl. Med.*, **2017**, *58*, 2010-2012.
[9] Nabati, M.; Salehi, H. *Iran. J. Org. Chem.*, **2017**, *9*, 2013-2023.
[10] Nabati, M. *Iran. J. Org. Chem.*, **2017**, *9*, 2045-2055.
[11] Nabati, M.; Kermanian, M.; Maghsoudloo-Mahalli, A.; Sarshar, S. *Iran. J. Org. Chem.*, **2017**, *9*, 2067-2077.
[12] Nabati, M.; Mohammadnejad-Mehrabani, H. *Iran. J. Org. Chem.*, **2017**, *9*, 2117-2121.
[13] Nabati, M.; Maghsoudloo-Mahalli, A. *Iran. J. Org. Chem.*, **2017**, *9*, 2239-2247.
[14] Nabati, M.; Maghsoudloo-Mahalli, A.; Mohammadnejad-Mehrabani, H.; Movahed-Tazehkand, H. *Iran. J. Org. Chem.*, **2018**, *10*, 2281-2285.
[15] Nabati, M. *Iran. J. Org. Chem.*, **2018**, *9*, 2291-2299.
[16] Blower, P. J.; Lewis, J. S.; Zweit, J. *Nucl. Med. Biol.*, **1996**, *23*, 957-980.
[17] Dutton, G. *Genet. Eng. Biotechn. N.*, **2015**, *35*, 10-11.
[18] Lange, R.; Heine, R.; Knapp, R.; deKlerk, J. M. H.; Bloemendal, H. J.; Hendrikse, N. H. *Bone*, **2016**, *91*, 159-179.
[19] Rashed, H. M.; Marzook, F. A.; Farag, H. *Radiol. Med.*, **2016**, *121*, 935-943.
[20] Mease, R.; Vaidyanathan, G.; McGougald, D.; Choi, J.; Chen, Y.; Shallal, H.; Brummet, M.; Shen, C.; Minn, I.; Kiess, A.; Sgouros, G.; Zalutsky, M.; Pomper, M. *J. Nucl. Med.*, **2016**, *57*, 14-33.
[21] Sarikavak, K.; Sevin, F. *Comput. Chem.*, **2017**, *5*, 145-158.
[22] Gijs, M.; Aerts, A.; Impens, N.; Baatout, S.; Luxen, A. *Nucl. Med. Biol.*, **2016**, *43*, 253-271.
[23] DeGraffenreid, A. J.; Feng, Y.; Barnes, C. L.; Ketring, A. R.; Cutler, C. S.; Jurisson, S. S. *Nucl. Med. Biol.*, **2016**, *43*, 288-295.

[24] Petrik, M.; Zhai, C.; Haas, H.; Decristoforo, C. *Clin. Transl. Imaging*, **2017**, *5*, 15-27.
[25] Kopka, K.; Benesova, M.; Barinka, C.; Haberkorn, U.; Babich, J. *J. Nucl. Med.*, **2017**, *58*, 17S-26S.
[26] Yadav, N.; Chuttani, K.; Mishra, A. K.; Singh, B. *J. Incl. Phenom. Macrocycl. Chem.*, **2015**, *83*, 299-307.
[27] Perils, J.; Cortezon-Tamarit, F.; Kuganathan, N.; Kociok-Kohn, G.; Dilworth, J. R.; Pascu, S. I. *Inorganica Chim. Acta*, **2018**, *475*, 142-149.
[28] Deri, M. A.; Ponnala, S.; Zeglis, B. M.; Pohi, G.; Dannenberg, J. J.; Lewis, J. S.; Francesconi, L. C. *J. Med. Chem.*, **2014**, *57*, 4849-4860.
[29] Adeowo, F. Y.; Honarparvar, B.; Skelton, A. A. *J. Phys. Chem. A*, **2017**, *121*, 6054-6062.
[30] Pijarowska-Kruszyna, J.; Karczmarczyk, U.; Jaron, A.; Laszuk, E.; Radzik, M.; Garnuszek, P.; Renata, M. *Nucl. Med. Rev.*, **2017**, *20*, 88-94.
[31] Martinez, T.; Gallego Peinado, M.; Sanchez Catalicio, J.; Perez Angel, F.; Contreras Gutierrez, J. *Nucl. Med. Commun.*, **2016**, *37*, 432-434.
[32] Uccelli, L.; Martini, P.; Pasquali, M.; Boschi, A. *J. Radioanal. Nucl. Chem.*, **2017**, *314*, 1177-1181.
[33] Suzuki, C.; Kimura, S.; Kosugi, M.; Magata, Y. *Nucl. Med. Biol.*, **2017**, *47*, 19-22.
[34] Yoo, J. R.; Heo, S. T.; Kim, M.; Kim, H. W.; Chang, J. W.; Song, H. *J. Infect. Dis.*, **2015**, *47*, 510-514.
[35] Fuente, A.; Zanca, R.; Boni, R.; Cataldi, A. G.; Sollini, M.; Lazzeri, E.; Mariani, G.; Erba, P. A. *J. Nucl. Med. Technol.*, **2017**, *45*, 236-240.
[36] Lezaic, L.; Socan, A.; Peitl, P. K.; Poglajen, G.; Sever, M.; Cukjati, M.; Carnelc, P.; Vrtovec, B. *Nucl. Med. Biol.*, **2016**, *43*, 410-414.
[37] Martinez, T.; Minara, E.; Martin-Falquina, T. C.; Fuente, T. *J. Label. Compd. Radiopharm.*, **2014**, *57*, 49-52.
[38] Meseguer-Olmo, L.; Montellano, A. J.;Martinez, T.; Martinez, C. M.; Revilla-Nuin, B.; Roldan, M.; Mora, C. F.; Lopez-Lucas, M. D.; Fuente, T. *Nucl. Med. Biol.*, **2017**, *46*, 36-42.
[39] Jean-Bay, E. *J. Neurosci. Nurs.*, **2000**, *32*, 169-176.
[40] Vries, E. F. J.; Roca, M.; Jamar, F.; Israel, O.; Signore, A. *J. Nucl. Med. Mol. Imaging*, **2010**, *37*, 848-848.
[41] Vanderghinste, D.; Eeckhoudt, M. V.; Terwinghe, C.; Mortelmans, L.; Bormans, G. M.; Verbruggen, A. M.; Vanbilloen, H. P. *J. Pharm. Biomed. Anal.*, **2003**, *32*, 679-685.
[42] Heilman, R. S.; Tikofsky, R. S.; Heertumz, R. V.; Coade, G.; Carretta, R.; Hoffmann, R. G. *Eur. J. Nucl. Med.*, **1994**, *21*, 306-313.
[43] Nabati, M. *J. Phys. Theor. Chem. IAU Iran*, **2017**, *14*, 49-61.
[44] Nabati, M. *J. Phys. Theor. Chem. IAU Iran*, **2016**, *13*, 133-146.
[45] Nabati, M.; Mahkam, M. *J. Phys. Theor. Chem. IAU Iran*, **2015**, *12*, 33-43.
[46] Nabati, M.; Mahkam, M. *Silicon*, **2016**, *8*, 461-465.
[47] Nabati, M.; Mahkam, M. *J. Phys. Theor. Chem. IAU Iran*, **2015**, *12*, 121-136.
[48] Nabati, M.; Mahkam, M.; Atani, Y. G. *J. Phys. Theor. Chem. IAU Iran*, **2016**, *13*, 35-59.
[49] Nabati, M.; Mahkam, M. *Org. Chem. Res.*, **2016**, *2*, 70-80.
[50] Nabati, M. *Chem. Method.*, **2017**, *2*, 128-146.
[51] Nabati, M.; Mahkam, M. *Inorg. Chem. Res.*, **2016**, *1*, 131-140.
[52] Nabati, M. *J. Phys. Theor. Chem. IAU Iran*, **2015**, *12*, 325-338.
[53] Frisch, M. J.; Trucks, G. W.; Schlegel, H. B.; Scuseria, G. E.; Robb, M. A.; Cheeseman, J. R.; Montgomery Jr., J. A.; Vreven, T.; Kudin, K. N.; Burant, J. C.; Millam, J. M.; Iyengar, S. S.; Tomasi, J.; Barone, V.; Mennucci, B.; Cossi, M.; Scalmani, G.; Rega, N.; Petersson, G. A.; Nakatsuji, H.; Hada, M.; Ehara, M.; Toyota, K.; Fukuda, R.; Hasegawa, J.; Ishida, M.; Nakajima, T.; Honda, Y.; Kitao, O.; Nakai, H.; Klene, M.; Li, X.; Knox, J. E.; Hratchian, H. P.; Cross, J. B.; Adamo, C.; Jaramillo, J.; Gomperts, R.; Stratmann, R. E.; Yazyev, O.; Austin, A. J.; Cammi, R.; Pomelli, C.; Ochterski, J. W.; Ayala, P. Y.; Morokuma, K.; Voth, G. A.; Salvador, P.; Dannenberg, J. J.; Zakrzewski, V. G.; Dapprich, S.; Daniels, A. D.; Strain, M. C.; Farkas, O.; Malick, D. K.; Rabuck, A. D.; Raghavachari, K.; Foresman, J. B.; Ortiz, J. V.; Cui, Q.; Baboul, A. G.; Clifford, S.; Cioslowski, J.; Stefanov, B. B.; Liu, G.; Liashenko, A; Piskorz, P.; Komaromi, I.; Martin, R. L.; Fox, D. J.; Keith, T.; Al-Laham, M. A.; Peng, C. Y.; Nanayakkara, A.; Challacombe, M.; Gill, P. M. W.; Johnson, B.; Chen, W.; Wong, M. W.; Gonzalez, C.; Pople, J. A. *Gaussian 03. Revision B.01*. Gaussian Inc. Wallingford. CT. **2004**.